Calibrating SPHERE, the exo-planet imager for the VLT

Francois Wildi[a1], David Mouillet[b], Jean-Luc Beuzit[b], Markus Feldt[c], Kjetil Dohlen[d], Thierry Fusco[e], Cyril Petit[e], Silvano Desidera[f], Raffaele Gratton[f], Hans-Martin Schmid[g], Maud Langlois[d], A .Vigan[d], Julien Charton[b], Riccardo Claudi[f], Ronald Roelfsema[h], Andrea Baruffolo[f], Pascal Puget[b]

[a] Observatoire de Genève, CH-1290 Sauverny, Switzerland
[b] Laboratoire d'Astrophysique de Grenoble, B.P. 53, F-38041 Grenoble Cedex 9, France
[c] Max Planck Institut für Astronomie, Königstuhl 17, D-69117 Heidelberg, Germany
[d] Laboratoire d'Astrophysique de Marseille, B.P. 8, F-13376 Marseille Cedex 12, France
[e] Office National d'Etudes et de Recherches Aérospatiales, B.P. 72, F-92322 Chatillon, France
[f] Osservatorio Astronomico di Padova, Vicolo dell'Osservatorio 5, I-35122 Padova, Italy
[g] Institute of Astronomy, ETH Zurich, CH-8092 Zurich, Switzerland
[h] ASTRON, P.O. Box 2, NL-7990 AA Dwingeloo, The Netherlands

ABSTRACT

One of the main challenges to obtain the contrast of >15mag targeted by an extra-solar planet imager like SPHERE lies in the calibration of all the different elements participating in the final performance. Starting with the calibration of the AO system and its three embedded loops, the calibration of the non-common path aberrations, the calibration of the NIR dual band imager, the NIR integral field spectrograph, the NIR spectrograph, the visible high accuracy polarimeter and the visible imager all require sophisticated calibration procedures. The calibration process requires a specific extensive calibration unit that provides the different sources across the spectrum (500-2320nm) with the stabilities and precisions required. This article addresses the challenges met by the hardware and the instrument software used for the calibration of SPHERE.

Keywords: exo-solar planets, extreme adaptive optics, coronagraphy, dual band imaging, polarimetry, spectral imaging

1. INTRODUCTION

The prime objective of the Spectro-Polarimetric High-contrast Exoplanet Research (SPHERE) instrument for the VLT is the discovery and study of new extra-solar giant planets orbiting nearby stars by direct imaging of their circumstellar environment. The challenge consists in the very large contrast between the host star and the planet, larger than 12.5 magnitudes (or 10^5 in flux ratio), at very small angular separations, typically inside the seeing halo. The design of SPHERE is optimized towards reaching the highest contrast in a limited field of view and at short distances from the central star. Both evolved and young planetary systems will be detected, respectively through their reflected light (mostly by visible differential polarimetry) and through the intrinsic planet emission (using IR differential imaging and integral field spectroscopy). The design of SPHERE and its expected performance has been the subject of prior publications [1], [3] and [4].

Calibration is of paramount importance to reach the expected high contrast of the instrument: Whether it is the extreme adaptive optics system which transfer functions must be determined for optimal dynamical performance, or the non-common path aberrations to reduce the static speckles of the optics, or more classically the detectors response, a maximal number of instrumental effects are measured to minimize their influence on the final performance. The number of calibration modes of SPHERE is almost tenfold larger than the operation modes.

[1] francois.wildi@unige.ch

2. DESCRIPTION OF SPHERE

SPHERE is divided into four subsystems: the Common Path and Infrastructure (CPI) and the three science channels, a differential imaging camera (IRDIS, InfraRed Dual Imaging Spectrograph), an Integral Field Spectrograph (IFS) and a visible imaging polarimeter (ZIMPOL, Zurich Imaging Polarimeter). The Common Path includes pupil stabilizing fore optics (tip-tilt and rotation), calibration units, the SAXO extreme adaptive optics system, and NIR and visible coronagraphic devices. ZIMPOL shares the visible channel with the wavefront sensor through a beamsplitter, which can be a grey (80% to ZIMPOL) beamsplitter, a dichroic beamsplitter, or a mirror (no ZIMPOL observations). IRDIS is the main science channel responsible for wide-field imaging in one or two simultaneous spectral bands or two orthogonal polarizations and low and medium resolution long slit spectroscopy. The IFS, working from 0.95 to 1.65 μm, provides low spectral resolution (R ~ 30) over a limited, 1.8" x 1.8", field-of-view. A photon sharing scheme has been agreed between IRDIS and IFS, allowing IFS to exploit the NIR range up to the J band, leaving the Hband, judged optimal for the DBI mode, for IRDIS for the main observation mode. This multiplexing optimizes the observational efficiency. The current implementation of SPHERE at the Nasmyth focus of the VLT is shown in Fig. 1 (R/h).

2.1 Common Path and Infrastructure (CPI)

The common pathis made of all the optics that supply the beam to the science channels: transfer optics, re-rotator, all elements of the adaptive optics (deformable mirrors, wavefront sensors, etc.) and coronagraphs. All these components are mounted on a large optical bench mounted on a triplet of active dampers, to which each science instrument will dock as a whole. When in operation on the Nasmyth platform A of the VLT UT3, SPHERE will be entirely enclosed in a thermal/dust cover and include a comprehensive automated cryo-vacuum system supplying 4 cryostats and a separate vacuum container .

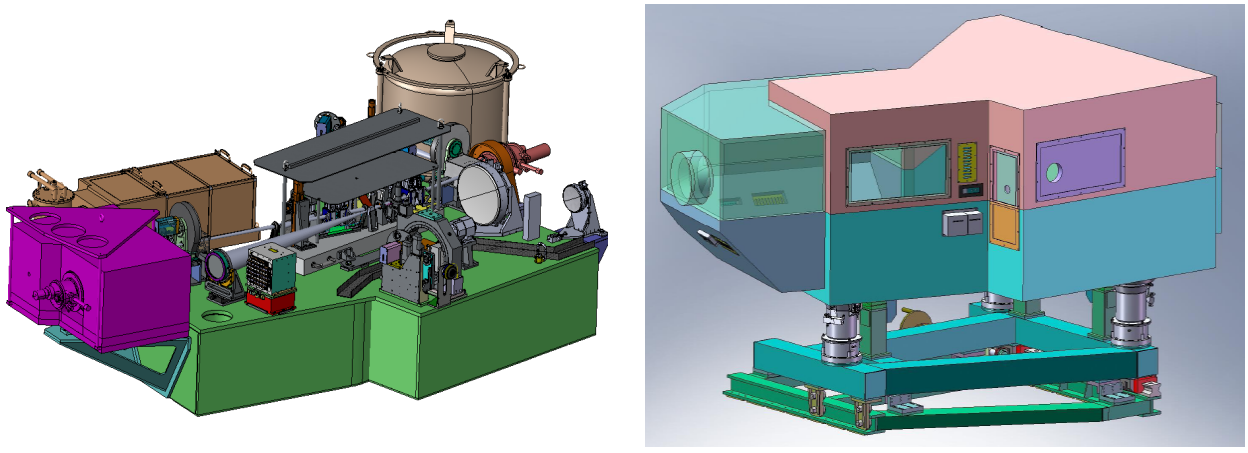

Fig. 1. The view on the left shows the complete SPHERE opto-mechanical assembly The view on the right shows how SPHERE will look like in operation, when the opto-mechanical assembly is mounted onto the vibration damping system and into the thermal-vacuum enclosure.

Extreme adaptive optics (SAXO)

Three loops and one off line calibration compose the SAXO extreme adaptive optics system.

- The main AO loop corrects for atmospheric, telescope and common path defects. The main impact is the increase of detection signal to noise ratio through the reduction of the smooth PSF halo due to turbulence effects.
- The Differential Tip-Tilt loop ensures a fine centering of the beam on the coronagraphic mask (correction of differential tip-tilt between VIS and IR channel). It will therefore ensure an optimal performance of the coronagraph device.
- The Pupil Tip-Tilt loop corrects for pupil shift (telescope and instrument). It will ensure that the uncorrected instrumental aberrations effects (in the focal plane) will always be located at the same position and thus will be canceled out by a clever post-processing procedure.
- Non-Common Path Aberrations will be measured with phase diversity, and their pre-compensation will lead to the reduction of persistent speckle.

The main AO loop uses a 41x41 actuator DM of 180 mm diameter, a high bandwidth (~1 kHz) tip-tilt mirror (TTM) with ±0.5 mas resolution and a 40x40 lenslet Shack-Hartmann wavefront sensor, covering the 0.45-0.95 µm, and equipped with a focal plane spatial filter[3] continuously variable in size from λ/d to 3λ/d at 0.7 µm, where d is the sub-aperture diameter, for aliasing control. It is based on a dedicated 240x240 pixel electron multiplying CCD runnig at 1200 fps.

2.2 IRDIS, the dual band imager and spectrograph

IRDIS design and performance predictions have been the subject to several communications (p. ex. [8], [9]). When SPHERE is in survey mode, IRDIS operates in dual band imaging (DBI) but it also has dual polarimetry and slit spectroscopy capability; using its dual filter wheel for simultaneous polarization measurements and its Lyot wheel to hold the dispersive elements for spectroscopy. IRDIS does not have calibration elements

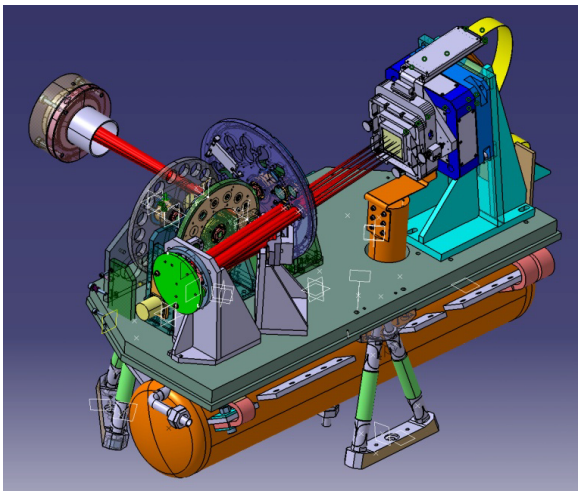

Fig 2: 3D view of the IRDIS opto-mechanics (w/o the surrounding cryostat). The dual beams produce their image on the same detector, located on a dithering stage on the right side of the bench.

2.3 IFS, the integral field spectrograph

To explore the innermost part of the science field, SPHERE has a spectro-imager called IFS. This instrument has a field of 145x145 pixels covering a 1.8 x 1.8 arcsec on the sky and can resolve the image spectrally with a resolution of 50 in the 0.95-1.35µm band or with a resolution of 30 in the 0.95-1.7 µm band [10], [11].

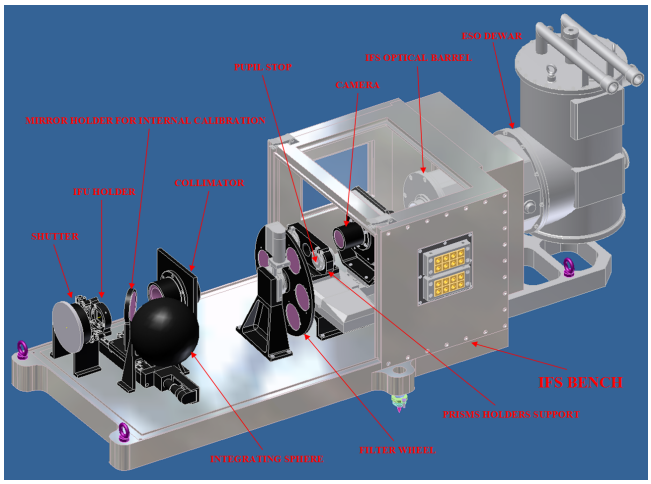

Fig 3: From the opto-mechanical point of view IFS is a relatively simple instrument: The IFU performs the spatial sampling of the field and the demagnification of the pixels. The light from each pixel is collimated, before going through the disperser. The disperser disperses the light from each pixel into a spectrum, which is imaged on the detector by the camera. Only the detector and the last lens are nitrogen cooled.

2.4 ZIMPOL, the Zurich IMaging POLarimeter

ZIMPOL (Zurich Imaging Polarimeter) is located behind SPHERE's visible coronagraph. This high precision polarimeter is based on a modulation / demodulation technique using a fast switching (1 kHz) ferroelectric liquid crystal polarization modulator and a special, demodulating CCD detector. Among its main specifications are a bandwidth of 500 to 900 nm and an instantaneous field of view of 3 x 3 arcsec^2 with access to a total field of view of 8 arcsec diameter by an internal field selector. The ZIMPOL optical train contains a common optical path that is split with the aid of a polarizing beamsplitter in two optical arms. Each arm has its own detector, but they are both located in the same cryostat and cooled to -80^{o}C. Above the beam splitter, the path contains common components for both arms like calibration components, common filters, a rotatable half wave plate and a ferroelectric liquid crystal polarization modulator. The two arms have the ability to measure simultaneously the two complementary polarization states in the same or in distinct filters. The images on both ZIMPOL detectors are Nyquist sampled at 600 nm.

The principle of ZIMPOL and its performance have been addressed in [12] and [13] respectively.

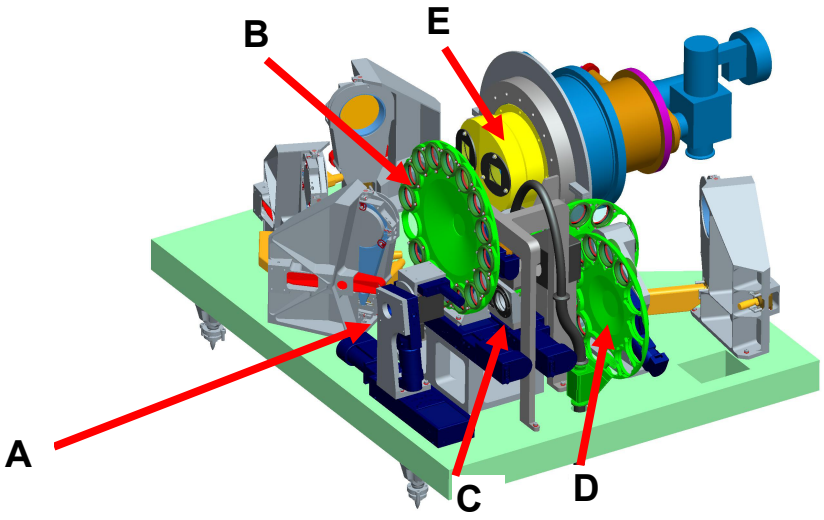

Fig 4: 3D view of ZIMPOL Opto-mechanics. A) polarization equalizer (1st optical component in the path), B) Calibration components wheel, C) ferroelectric liquid crystal (FLC) modulator which is the center piece of the ZIMPOL system, D) 2 other wheels allow different bands to be measured simultaneously in the 2 arms, E) Cryostat holding the 2 detectors for the 2 arms.

3. CALIBRATION REQUIREMENTS

3.1 Detectors

SPHERE uses 2 infrared science detectors, 2 visible science detector (both for ZIMPOL), one visible and one infrared wavefront sensing detectors. All these detectors need classical dark fielding, and flat fielding. In general it is requested that the detectors be flat fielded with fluxes commensurate to the ones expected during operation. I.e. that the exposures last no more than 10s.

High contract imaging put severe constraints on the flatness on the flat field: The most stringent requirement coming from the DBI is 99.9% homogeneity from pixel to pixel and 99.9% homogeneity within a 10x10 pixel area

3.2 Adaptive optics, coronagraphs

The adaptive optics loops require a significant number of calibrations: Wavefront sensor zero, interaction matrices (the measurement of the relationship between actuator activation and sensor measurement) have to be measured between the high order DM and the main visible wavefront sensor, between the fast image tip-tilt mirror and the main visible wavefront sensor, between the differential tip-tilt plate and the differential tip-tilt sensor, and between the pupil tracking mirror and the visible wavefront sensor.

All in all AO requires a significant number of calibrations, but they do not put strong constraints on the calibration hardware: Point sources of sufficient flux will do the job. With 1350 sub-apertures, read at 1200 fps, each requiring 1000 detected photo-electrons; this does indeed mean 10^{10} ph/s entering the system.

3.3 Coronagraphs

Coronagraphs require calibration in the sense that the high contrast imagery depends very much on the ability of the AO to reach the highest correction on the coronagraphic focal mask. There are 2 parts in the correction error: a dynamic part due to the atmospheric turbulence and a static part due to the presence of static aberrations in the corrected wavefront. These static aberrations can be removed by calibration which leads to a significant reduction of the static speckles.

To this purpose, the wavefront error (WFE) from the input focus to the Lyot focal mask must be measured. However, this error cannot be measured directly because there is not sensor at the location of the focal mask. It is computed by subtraction of 2 measurements: The WFE map of IRDIS is measured by phase diversity using a double source just before the coronagraphic focal plane. Then, the WFE map of the total infrared path to IRDIS is measured by phase diversity and a source in the SPHERE input focal plane. The WFE map to the coronagraph is the difference between the 2. See fig 5 below. This WFE map is used to produce a set of numerical offsets that are introduced to bias the output of the wavefront sensor so as to produce the best possible wavefront not on the wavefront sensor channel but on the coronagraph channel

The same scheme is applied to calibrate the wavefront error to the visible coronagraph, using ZIMPOL for the measurement by phase diversity. Of course, the calibrations for the NIR or the visible are not simultaneous. NIR and VIS science channels are never working together in SPHERE.

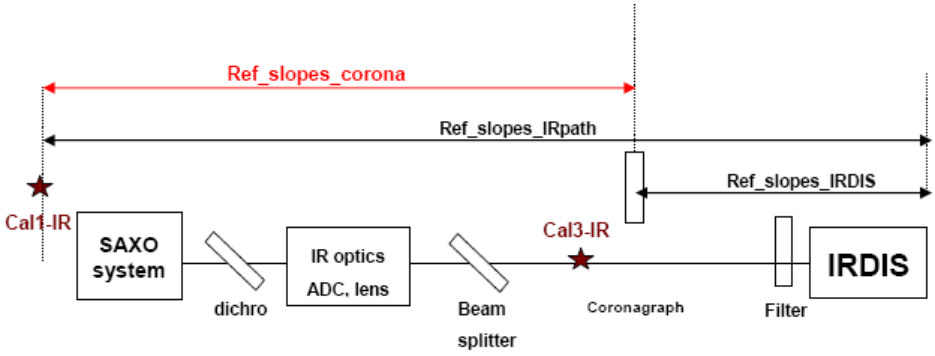

Fig 5: The calibration of the wavefront error (WFE) to the coronagraph is made by subtracting the IRDIS WFE (from the coronagraph) to the total NIR WFE

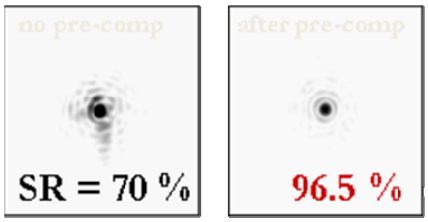

@ 633nm

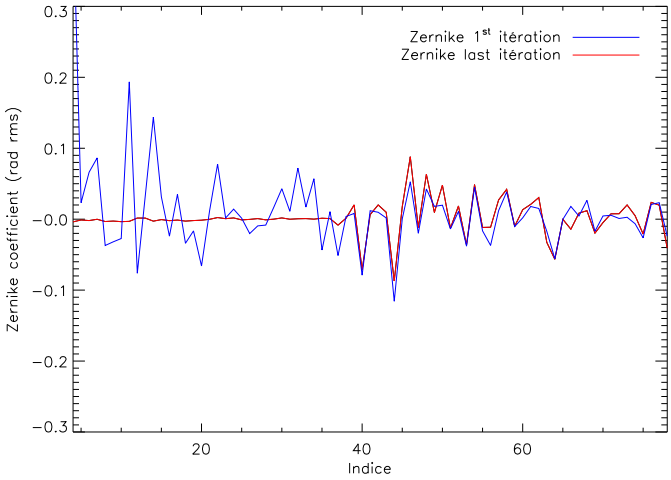

Fig 6: Results showing the quality of WFE improvement obtained by pre-compensation based on the measurement of WFE by phase diversity measured on an experimental bench at ONERA.

Given that SPHERE has two Atmospheric Dispersion Correctors (ADC, one for the NIR channel and one for the VIS channel), this calibration must be repeated for various ADC positions.

This calibration requires diffraction limited sources throughout the science channels spectra with sufficient throughput for high SNR imaging of defocused images.

3.4 Imaging

The calibration of SPHERE also requires that a wide spectrum source is available for the characterization of the field distortion. This source must have an accuracy of +/- 0.5 milli arcsecond (mas)

The calibration of SPHERE also requires that unresolved (i.e. point) sources are available for the characterization of the ghosts. These sources are also use to test

3.5 Spectroscopy

Whether this is integral field spectroscopy with the IFS of slit spectroscopy with IRDIS, spectroscopy requires wavelength calibration sources. The constraints here come from the wavelength range on one side and the low resolution on the other side. Traditional spectral lamps have a much too dense set of lines that cannot be resolved by the low resolution spectroscopy. The gap required for a Fabry-Perot etalon would correspond to a few waves (i.e <10 micron) which is both too thin to guarantee a manufacturable air-spaced etalon and too thick for a thin film deposited one, because of the stress induced within the thin film. Given the resolution of the spectroscopic modes (from 30 for the lowest resolution IFS mode to 500 for IRDIS highest resolution), a stability of 0.05nm over the instrument lifetime is required.

3.6 Polarimetry

An extra-solar planet is expected to produce a very weak localized polarization signal on top of the smoothly distributed polarization signal of the PSF from the bright parent star. Thereby the light of the parent star can be used a zero polarization reference target. It is expected that a typical planet detection, the primary science case, has a low signal to noise ratio of about S/N = 3 to 20. For other scientific applications a higher precision is desirable. The calibration of the polarimetric mode requires therefore: (a) the possibility to disentangle a very weak point-like polarization flux signal which is 10^5 times weaker than the PSF intensity from any spurious (instrumental or atmospheric) polarization features, (b) the possibility to measure extended polarization signals, e.g. scattered light from disk, with a polarization flux which is 10^3 times less than the PSF intensity (c) a determination of the zero point of the polarization position angle with a precision of a 1 to 3 degrees, (d) knowledge of the polarimetric efficiency with a precision of a few %.

The requirements (a) and (b) are very demanding and besides a good calibration they require as prerequisite a very sophisticated polarimetric measuring strategy. The ZIMPOL polarimeter (single beam - fast modulation / demodulation) is a measuring principle which is in a certain sense ``self-calibrating''. For example no (intensity) flat-field calibrations are required thanks to the special differential measuring technique employed.

4. CALIBRATION HARDWARE DESIGN

The design of the calibration hardware must be compatible with the environmental constraints at the telescope, two which are of importance to us:

- The temperature of SPHERE is uncontrolled. The temperature at the VLT can vary between 0C and 15C. On the other hand, within the SPHERE thermal enclosure, the temperature of any component cannot be different by more than 0.4C from the ambient.
- The telescope chamber is inaccessible during the night.

4.1 Concept

The calibration unit is built in two parts: on one side a source unit is hosting the sources proper and their electronics. On the other side, a feed unit feeds SPHERE with the light from the sources. The source unit features lasers, a lamp with two incandescent bulbs in cold redundancy, conditioning optics, a filter wheel and a linear stage where different fibers can be fed by the lamp.

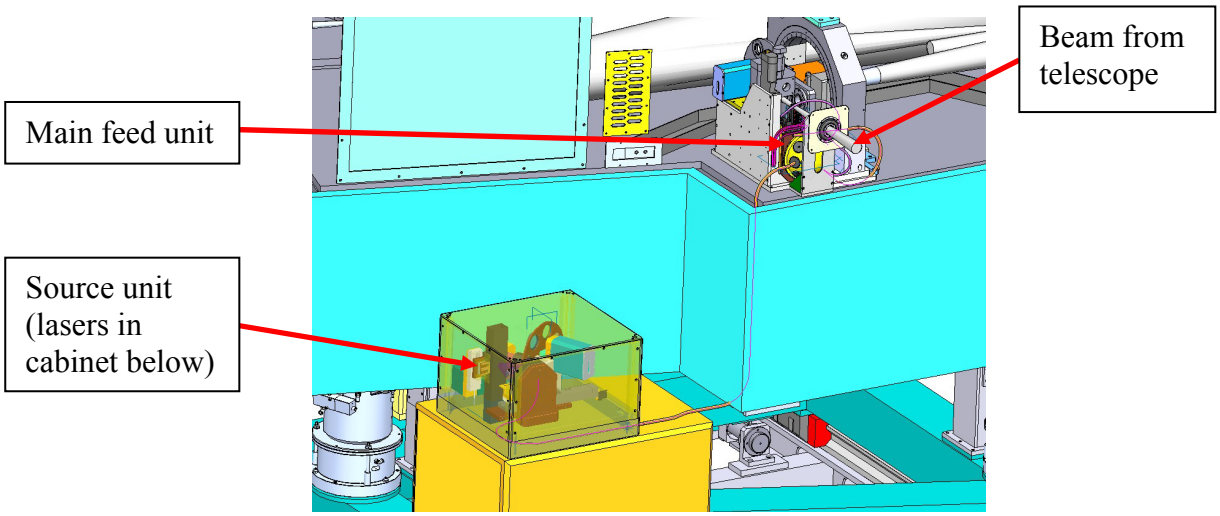

Fig 7: 3D view of the calibration unit installed on SPHERE. The source unit sits outside the thermal/dust enclosure for thermal reasons. The main feed unit is located between the entrance window and the retractable half wave plate #1used for polarization compensation.

4.2 Detectors

The requirements applicable to the flat field are somewhat contradictory: on one side this must be very homogenous and on the other side it must be bright (i.e. high radiance). As shown in the equation below, the radiance produced by an integrating sphere is proportional to the inverse of the diameter, while as shown on fig 8, the radiance emitted by one pixel is the integral of the intensity emitted by each element of the sphere surface inside the aperture cone of the instrument. Therefore, the larger the sphere, the larger the surface over which we integrate and the better the averaging of the intensity.

The radiance at the output port of an integrating sphere can be described by

$$L = \frac{\Phi_i}{\pi A_s} \cdot \underbrace{\frac{\rho}{1-\rho(1-f)}}_{M} \qquad \text{With} \qquad f = \frac{A_{input} + A_{exit}}{A_s}$$

Φ_i is the input flux, A_s is the integrating sphere surface, ρ is the reflectance of the internal wall of the sphere, A_{input}, A_{exit} and A_s are the input port(s) surface, the exit port surface and the internal surface of the IS respectively.

Due to size constraints in SPHERE, the integrating sphere inside diameter had to be limited to 120mm, which is less than originally planned. To mitigate the risk that the homogeneity obtained is not within the requirements we have designed a slightly oversize output port in the integrating sphere so that we can dither the sphere while flat fielding.

The broadband source chosen is an incandescent lamp which, of course, because of the thermal constraints, cannot be located inside the sphere. Therefore a light guide needs to bring the light from the lamp to the integrating sphere. The etendue of this light guide is dimensioned to allow the necessary flux to be brought to the sphere.

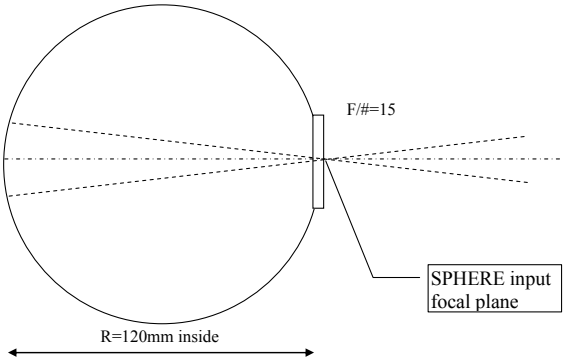

Fig 8: A large integrating sphere helps defocusing the internal side of the sphere as seen by the instrument and homogenizes the flat field at high spatial frequencies. If the diameter is large, the footprint of the beam at the back of the sphere is mostly the same for 2 adjacent pixels.

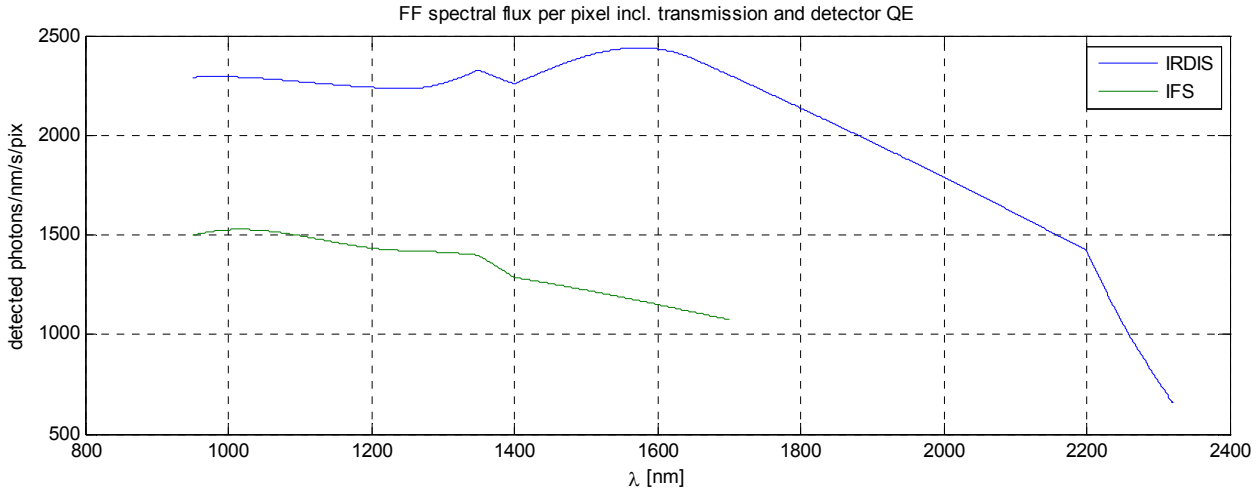

Fig 9: The spectral flux per pixel from the flat field calibration source expected at the detector level (including SPHERE transmission and detector QE). To get the full flux this value must be multiplied by the science channel filter bandwidth. The cut-off beyond 2200nm is due the behavior of the silica fiber bundle linking the source to the feed units.

4.3 Imaging + AO

Point sources must be available. Their size must be <λ/2D, to be unresolved on the detector. These sources are made of monomode optical fibers. To optimize to flux and the homogeneity, 3 different fibers cover the wavelength range, with a special fluoride fiber covering the K-band.

These source are used both to calibrate the ghosts and to estimate the system performance

To be able to run the AO system at full speed, the incandescent source is supplemented with a visible laser, so that the flux is sufficient. Depending on the fiber, the laser beam will not be monomode, but this will not impact the wavefront sensor which resolution is λ/d, where d is the diameter of a subaperture. d = D/40.

4.4 Coronagraphs

The measurement of non-common path aberrations by phase diversity requires a double source paced in the vicinity of the coronagraphic focal planes. These sources are made of photonic crystal fibers (PCF) fed by the incandescent lamp. This guaranties a diffraction limited monomode spot throughout the wavelength range; a solution that can only be applied at these slow (F/40 in the NIR and F/30 in the VIS) intermediate foci, due to the low NA of these PCF fibers.

4.5 Spectroscopy

The solution chosen to produce the spectral features required for the spectral calibration of the spectrographic modes is to use single mode distributed fiber Bragg grating (DBG) laser diode. With a typical linewidth <0.01nm these lasers are much below the resolution limit of the spectroscopic modes. Experience shows that the stability of these devices, when properly temperature and power controlled is 10 GHz, or 0.03 nm @ 1000nm. A set of 6 lines with approximately equal spectral separation has been selected from off-the-shelf laser diodes.

Since the SPHERE IFS performs integral field spectroscopy, the spectral sources needs to cover the field of view (FOV) of this science channel. The same is true for IRDIS, where the slit of the spectrograph samples its complete FOV in one direction. This is why our DBG laser diodes are fiber coupled to the integrating sphere.

To determine the LSF of IRDIS in spectroscopic mode, part of the light of 2 spectral lines is coupled to a single mode fiber forming an unresolved spectral source.

4.6 Polarimetry

ZIMPOL measures the polarization at the position of the fast modulator. The measured polarization is therefore composed of the polarization from the target (sky) and all the polarization effects introduced by the optical components in front of the polarization modulator. Thus the measurements must be calibrated for all the polarization effects introduced by the telescope and instrument. This includes the polarization from strongly inclined mirrors like the telescope mirror M3 (Nasmyth) of the telescope and a derotator. For the polarimetric calibration the instrument is divided into three sections: (a) the telescope, (b) the derotator, the AO part, the coronagraph, and (c) ZIMPOL. Each of these sections can be calibrated separately. The sections (b) and (c) have their own insertable calibration components (linear polarizer, quarter wave retarder plate, and circular polarizer) for the determination of the instrument polarization and the polarization cross talks. These calibrations can be carried out during daytime with the flat field source located inside SPHERE. The calibration of the telescope polarization has to be carried out with night time observations of polarization standard stars.

In addition a polarization switch (rotatable achromatic half wave retarder plate) can be inserted just after the telescope and the telescope polarization compensator system. This switch can reverse the polarization signal of consecutive observations. This allows to disentangle with high precision the target polarization (including the polarization effects of the telescope) from the instrument polarization introduced by all the components (derotator, AO-system, coronagraph, ZIMPOL) located after the switch. This device should allow an accurate self-calibration of the polarization effect introduced by the instrument.

5. IMPLEMENTATION

A single lamp with a incandescent lamp is used for all sources but the spectral ones. It is equipped with a source selector stage, a bulb exchange stage (for redundancy) and a neutral density filter wheel. Inside SPHERE, the main feed unit features 3 broad band point sources, a spectral point source to measure the spectrographs LSF, the flat filed source and the distortion calibration mask. A linear stage allows refocusing when polarization components are introduced in the optical train.

The redundancy provided by the spare bulb is required to guarantee a maximal reliability. Indeed the flat fielding requirements are so tight, in particular for the integral field spectroscopy, that flat filed exposures must be taken in-between science exposures, when the telescope is repointing.

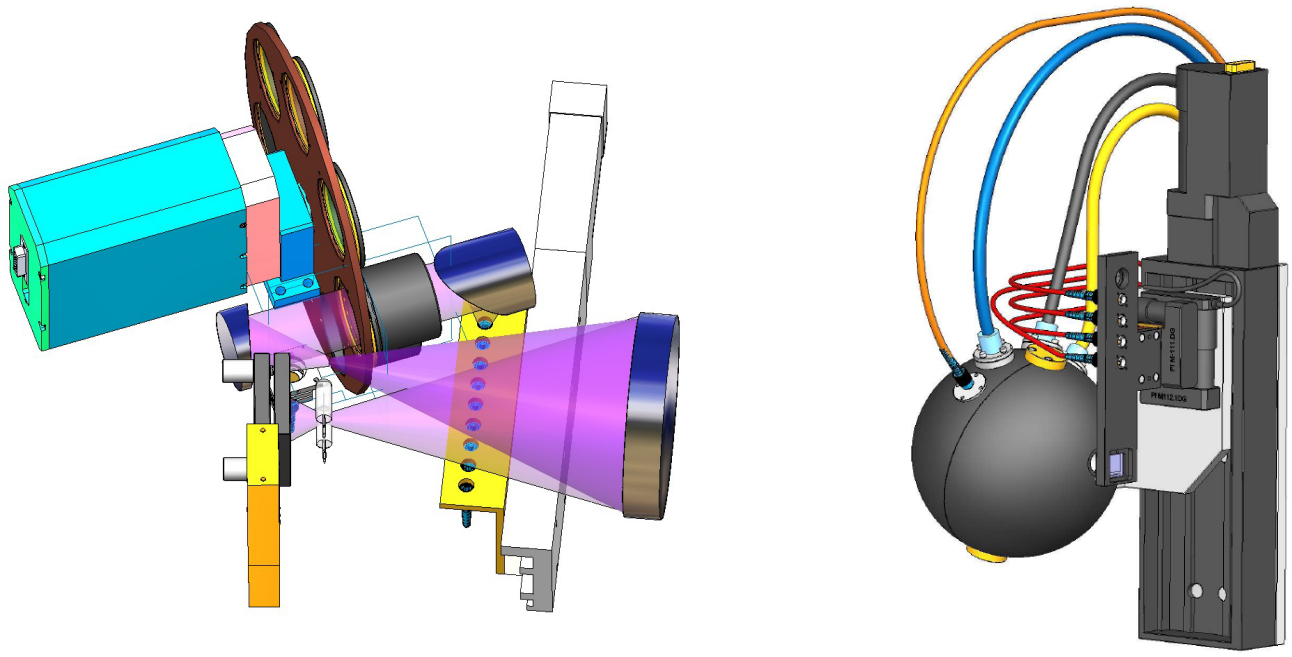

Fig 10: 3D views of the source unit (L/h) and the main feed nuit (R/h) of the calibration module. The point sources on the feed unit are mounted on an horizontal stage to allow re-focusing when the polarization components are inserted in the beam, which changes the location of the SPHERE input object point

6. CONCLUSION

The performance of a high contrast imager like SPHERE depends crucially on the calibration of the different instrumental artifacts. In our case the complexity of the calibration is significant and required a significant effort in terms of definition, requirements collection and design. The calibration of SPHERE involves 12 motors, 9 different light sources, an extensive control system and it makes up 90 instrument modes while the operation modes total only 11!

The SPHERE calibration module development follows the general SPHERE schedule. Its manufacturing phase is now nearing completion and the hardware integration and test phase should be complete by the end of 2009, in time for this unit to be used for the calibration all SPHERE sub-systems during final integration.

REFERENCES

[1] F. Wildi, J.-L. Beuzit, M. Feldt, D. Mouillet, K. Dohlen, P. Puget, A. Baruffolo, J. Charton, P. Baudoz, A. Boccaletti, L. Abe, R. Claudi, Ph. Feautrier, T. Fusco, R. Gratton, N. Hubin, M. Kasper, M. Langlois, R. Lenzen, A. Pavlov, C. Petit, J. Pragt, P. Rabou, R. Roelfsema, M. Saisse, H.-M. Schmid, E. Stadler, M. Turatto, S. Udry, R. Waters, T. Henning, A.-M. Lagrange, F. Vakili. "SPHERE: The VLT exo-planet imager in the post-FDR phase", *Techniques and Instrumentation for Detection of Exoplanets IV*, SPIE 7440-24 (2009)

[2] Jean-Luc Beuzit, Markus Feldt, Kjetil Dohlen, David Mouillet, Pascal Puget, Francois Wildi, L. Abe, J. Antichi, A. Baruffolo, P. Baudoz, A. Boccaletti, M. Carbillet, J. Charton, R. Claudi, M. Downing, C. Fabron, Ph. Feautrier, E. Fedrigo, T. Fusco, J.-L. Gach, R. Gratton, T. Henning, N. Hubin, F. Joos, M. Kasper, M. Langlois, R. Lenzen, C. Moutou, A. Pavlov, C. Petit, J. Pragt, P. Rabou, F. Rigal, R. Roelfsema, G. Rousset, M. Saisse, H.-M. Schmid, E. Stadler, Ch. Thalmann, M. Turatto, S. Udry, F. Vakili, R. Waters, "SPHERE: a 'Planet Finder' instrument for the VLT", *Ground-based and Airborne Instrumentation for Astronomy II*, SPIE 7014-42 (2008)

[3] F. Wildi, J.-L. Beuzit, M. Feldt, D. Mouillet, K. Dohlen, P. Puget, A. Baruffolo, J. Charton, J. Antichi, P. Baudoz, A. Boccaletti, M. Carbillet, R. Claudi, Ph. Feautrier, E. Fedrigo, T. Fusco, R. Gratton, N. Hubin, M. Kasper, M. Langlois, R. Lenzen, C. Moutou, A. Pavlov, C. Petit, J. Pragt, P. Rabou, R. Roelfsema, M. Saisse, H.-M. Schmid, E. Stadler, Ch. Thalmann, M. Turatto, S. Udry, R. Waters, T. Henning , A.-M. Lagrange , F. Vakili., "The SPHERE

exoplanet imager: Status report at PDR", *Astronomical Adaptive Optics Systems and Applications III*, SPIE 6691-18 (2007)

[4] K. Dohlen, JL Beuzit, M. Feldt, D. Mouillet, P. Puget, F. Wildi, J. Charton , C. Moutou, A. Longmore, T. Fusco. A. Boccaletti, P. Baudoz, P. Rabou, Ph. Feautrier, M. Langlois, M. Saisse, R. Gratton, J. Antici, A. Berton, HM. Schmid , R.Waters, "SPHERE, a planet finder instrument for the VLT." in *Ground-based and Airborne Instrumentation for Astronomy*. SPIE 6269 (2006)

[5] Anthony Boccaletti "Prototyping achromatic coronagraphs for exoplanet characterization with SPHERE", in *Adaptive Optics Systems*, SPIE 7015-46 (2008)

[6] G. Guerri, S. Robbe-Dubois, J.-B. Daban, L. Abe, R. Douet, Ph. Bendjoya, F. Vakili, M. Carbillet, "Apodized Lyot coronagraph for the VLT instrument SPHERE: laboratory tests and performances of a first prototype in the visible", in *Ground-based and Airborne Instrumentation for Astronomy II*, SPIE 7014-124 (2008)

[7] C. Petit, T. Fusco, J.-M. Conan, J.-F. Sauvage, G. Rousset., P. Gigan, J. Charton, D. Mouillet, P. Rabou, M. Kasper, E. Fedrigo, N. Hubin, Ph. Feautrier, J.-L. Beuzit, P. Puget, "The SPHERE XAO system: design and performance", in *Adaptive Optics Systems*, SPIE 7015-65 (2008)

[8] K. Dohlen, M. Langlois, M. Saisse, L. Hill, A. Origne, M. Jacquet, Ch. Fabron, J.-C. Blanc, M. Llored, M. Carle, C. Moutou, A. Vigan, A. Boccaletti, M. Carbillet, D. Mouillet, J.-L. Beuzit "The infrared dual imaging and spectrograph for SPHERE: design and performance", in *Ground-based and Airborne Instrumentation for Astronomy II*, SPIE 7014-126 (2008)

[9] A. Vigan and M. Langlois and C. Moutou and K. Dohlen, "Long slit spectroscopy for exoplanet characterization in SPHERE", *Ground-based and Airborne Instrumentation for Astronomy II.* , SPIE, 7014-

[10] R.. Claudi, M. Turatto, R. Gratton, J. Antichi,; E. Cascone,; V. De Caprio,; S. Desidera, D. Mesa, S. Scuderi, "SPHERE IFS: the spectro differential imager of the VLT for exoplanets search", in *Ground-based and Airborne Instrumentation for Astronomy II*, SPIE 7014-119 (2008)

[11] S. Desidera, R. Gratton, R. Claudi, J. Antichi, D. Mesa, M. Turatto,; P. Bruno, E. Cascone,; V. De Caprio, E. Giro; S. Scuderi; M. Feldt, A. Pavlov, K. Dohlen, J-L Beuzit, D. Mouillet, P. Puget, F. Wildi, "Calibration and data reduction for planet detection with SPHERE-IFS", in *Ground-based and Airborne Instrumentation for Astronomy II*, SPIE 7014-127 (2008)

[12] D. Gisler, H.M. Schmid, C. Thalmann, H.P. Povel, J.O. Stenflo, F. Joos, M. Feldt, R. Lenzen, J. Tinbergen, R. Gratton, R. Stuik, D.M. Stam, W. Brandner, S. Hippler, M. Turatto, R. Neuhäuser, C. Dominik, A. Hatzes, Th. Henning, J. Lima, A. Quirrenbach, L.B.F.M. Waters, G. Wuchterl, H. Zinnecker, "CHEOPS/ZIMPOL: a VLT instrument study for the polarimetric search of scattered light from extrasolar planets", in: *Ground-based instrumentation for astronomy*, SPIE 5492-463 (2004)

[13] Ch. Thalmann, H.-M. Schmid, A. Boccaletti, D. Mouillet, K. Dohlen, R. Roelfsema, M. Carbillet, D. Gisler, J.-L. Beuzit, M. Feldt, R. Gratton, F. Joos, Ch. U. Keller, J. Kragt, J. H. Pragt, P. Puget, F. Rigal, F. Snik, R. Waters, F. Wildi, "SPHERE ZIMPOL: Overview and performance simulation", in *Ground-based and Airborne Instrumentation for Astronomy II*, SPIE 7014-120 (2008)